ISSN : 0974 - 7494 Volume 5 Issue 3,4

Trade Science Inc.

Nano Science and Nano Technology
An Indian Journal

Full Paper

NSNTAIJ, 5(3,4), 2011 [140-146]

Dynamic properties of quasi-one dimensional spin nanocontact

Rachid Rabhi[1], Boualem Bourahla[1,2*], Ouahiba Nafa[1], Rachid Tigrine[2]

[1]Laboratory of Physics and Quanta Chemistry, M. Mammeri University, BP17 RP, Tizi Ouzou, (ALGERIA)

[2]Laboratory of Physics and Condensed State UMR 6087, University of Maine, Le Mans, (FRANCE)

E-mail : bourahla_boualem@yahoo.fr

PACS: 75.30.Ds; 75.30.Fv; 75.40.Gb; 75.40.Mg

Received: 4th December, 2011 ; Accepted: 26th December, 2011

ABSTRACT

We investigate the scattering phenomena at the inhomogeneous boundary of an atomic nanocontact in quasi-one dimensional magnetic structure. In particular, we study an atomic nanocontact separating two waveguide groups of semi-infinite spin ordered ferromagnetic monatomic chains. The model system is supported on a non-magnetic substrate and considered otherwise free from magnetic interactions. The spin dynamics of the quasi-one dimensional system is studied by the matching method, the coherent magnon transmission, magnonic conductance and the magnetic localized states are calculated and analyzed. The inter-atomic magnetic exchange is varied on the nanocontact domain to investigate the consequences of magnetic softening and hardening for the calculated properties. The numerical results show the interference effects between the incident magnons and the localized spin states on the nanocontact domain, with characteristic Fano resonances. The results yield an understanding for the relation between the coherent magnon conductance and the spin nanocontact in the perfect quasi-one dimensional ferromagnetic structure.

KEYWORDS

Spinwaves;
Atomic nanocontact;
Fano resonances;
Localized states.

INTRODUCTION

The physics of low-dimensional magnetic systems has been of interest for some time but particularly significant progress, both in experiment and theory, has been made during the last several years. Related research activities have been growing because the quantum nature of low-dimensional low-spin systems promises a rich variety of phenomena to be explored. Among other features, the transport of energy in 1D-magnetic systems is expected to be highly unusual. A number of models describing 1D-dimensional systems are integrable, implying, for instance, conservation of energy current and, as a consequence, ballistic energy propagation and divergent thermal conductivity. The question of whether the energy transport is diffusive or ballistic is currently under active discussion for atomic[1, 2] as well as spin[3, 4] 1D-systems.

The presence of atomic defect in magnetically ordered systems affects essentially the magnon spectrum leading to the appearance of new modes outside the bulk band of an ideal system. These modes are named

localized states and are strongly depending on the nature of the structure defect (such as atomic steps, adatoms, surface, interface, irregular distribution, atomic hole defect...). There is an increasing volume of experimental data and findings to elucidate the structural[5-8] and magnetic[9-11], properties of systems containing atomic defect or nanostructures. Consequently, there are a number of theoretical methods to deal with the effects of different type of atomic defects[12]. The principal mathematical formulation used to describe, for example, the spin motion equation, in Heisenberg systems[13], is based on the Green functions method, which can give information on the magnetic properties at the crystal defect, the spectral densities and the thermodynamic properties of different systems[14, 15].

In this work, we present a model to study spinwaves transmission via an atomic nanocontact in quasi-1D system, which is considered to act as a magnetic joint between two groups of semi-infinite magnetically ordered Heisenberg monatomic chains.

The system is supported on a non-magnetic substrate, and considered otherwise as free from magnetic interactions with his environment. The dynamics of spins and the magnon diffusion, which are the magnetic excitations on the chains in the presence of the nanocontact, is the subject of our analysis. The coefficients of transmission and reflection, magnonic conductance and localized spin states are derived as elements of a Landauer-type scattering matrix. The purpose is to give a theory of the properties of a spin nanocontact and an understanding of the relation between the coherent magnon conductance via the nanocontact, and the structural configuration of the latter. We examine three different cases concerning the magnetic exchange in the nanocontact zone. This makes it possible to know the influence of softening and hardening of the magnetic exchange in the nanocontact domain on the magnetic properties.

In the next section we present the basic elements of the model, describing the spin dynamics on the group of monatomic chains that constitute a quasi-one-dimensional crystallographic waveguide, on either side of the nanocontact domain. In section 3, we study the spin dynamics of the nanocontact itself. The individual and the total transmission are then derived using the matching method[16-19]. In section 4 numerical applications are presented for the spin nanocontact to illustrate the considered model. Conclusions are also presented and discussed in this section.

THEORETICAL MODEL

The structural configuration studied in this paper, for the magnon conductance via atomic nanocontact, is presented in Figure 1. The lattice consists of two identical groups of four semi-infinite monatomic chains disposed in the space as quasi-one dimensional input and output waveguides.

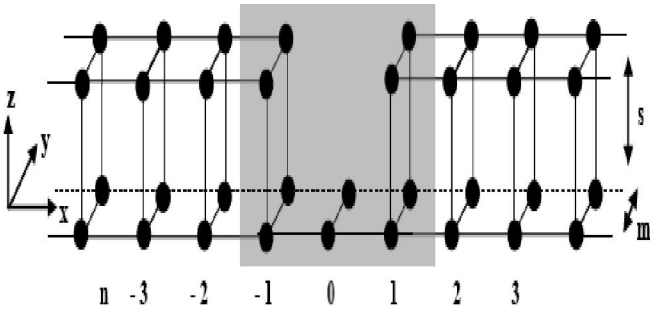

Figure 1 : A schematic representation of the quasi-1D crystallographic waveguides with an atomic nanocontact as a joint between them. The quasi-one-dimensional waveguides are made up from four semi-infinite monatomic chains disposed in the space. The shaded zone denotes an effective nanocontact domain.

The integral of exchange between nearest neighbors in the domains to the left and the right of the nanocontact zone are represented respectively by the constants J, where the shaded area in Figure 1, constitutes the effective nanocontact domain. The integral of exchange in this inhomogeneous boundary may differ from perfect zone value, and are hence labeled J_d. It is convenient next to define the following ratio:

$$\gamma = J_d / J \qquad (1)$$

For ferromagnetic Heisenberg exchange interactions between nearest neighbors, the Hamiltonian of the ground state is given by

$$\mathbf{H} = -2 \sum_{p \neq p'} J_{pp'} \mathbf{S}_p \cdot \mathbf{S}_{p'} \qquad (2)$$

S_p ($S_{p'}$) are the spin vectors, where $p \equiv$ (n, m, s) along the x, y and z directions, respectively. The exchange constants $J_{pp'} = J$ coupling magnetically nearest neighbor sites p (p') in the system are the same everywhere except on the nanocontact domain.

The three cases analyzed for the studied nanocontact are characterized by the following possibilities

Full Paper

$\gamma < 1, \gamma = 1$ and $\gamma > 1$ (3)

For $\gamma < 1$ and $\gamma > 1$, a magnetic softening or hardening is said to take place on the nanocontact domain. For $\gamma = 1$ the same exchange interactions exist throughout the system. It is also assumed that the exchange is homogeneous between the sites of the quasi-1D system.

Consider the spin precession displacements $\zeta^{\pm}_{p}(t)$, where $\zeta_{p}\alpha(t) = S_{p}\alpha(t) - < S_{p}\alpha >$, the brackets are thermal averages. α denotes the Cartesian directions, $\alpha = z$ is normal to the substrate. The method employed to study the spin dynamics, may be described by the equations of motion for the spin precession displacements on atomic sites *p*, see Ref.20 for details.

Suppose that the sites *p* are distant from the nanocontact domain, such that $p \equiv (n, m, s)$, the equations for spin dynamics to the left and right of the shaded domain in Figure 1, may be cast in the matrix form

$$[I - D(\eta)] |^{\pm}_{p} > = 0 \quad (4)$$

$\Omega = \omega/\omega_0 = \hbar\ \omega/2JS$ is a dimensionless frequency for the perfect quasi-1D magnetically ordered waveguides. *I* denotes a unit matrix, and $D(\eta)$ is a spin dynamics matrix characteristic of the perfect waveguide. η is a generic phase factor between neighboring sites on the waveguide along the axis in the x-direction.

In this representation $|\zeta^{\pm}_{p} >$ is the corresponding vector of the spin fluctuations for the column of the magnetically ordered waveguide, made up of the four magnetic monatomic chains, disposed in the space. $[\Omega I - D()]$ is an irreducible four by four matrix for the four inequivalent sites per unit cell. Both the propagating and the evanescent eigenmodes are described by the phase factor doublets $\{\eta, \eta^{-1}\}$.

The propagating magnon modes are determined by the condition that $|\eta| = 1$, whereas the evanescent modes are determined from the condition $|\eta| < 1$[16-19]. The exact solutions for each doublet are obtained as a function of the frequencies Ω. These solutions are obtained when the secular equation of the spin dynamic matrix $[\Omega I - D(\eta)]$ vanishes. For the system under study the secular equation may be expressed as a polynomial of degree eight in η

$$\Sigma A_{s}(\Omega)\, \eta^{s} = 0 \quad (5)$$

$A_{s}(\Omega)$ are the polynomial coefficients. Due to the Hermitian nature of the spin dynamics in the absence of strong external magnetic fields, both phase factors $\{\eta, \eta^{-1}\}$ verify symmetrically the polynomial forms.

The solutions of Eq.(5) provide the eigenmodes of the system. There are, however, only four modes of physical interest. For the propagating modes η_i, their inverse η_i^{-1} are modes propagating in the opposite sense and both represent the magnon dispersion branches. For the non propagating modes only the evanescent modes $|\eta_i| < 1$ are considered, their inverse representing non physical divergent modes.

The magnons dispersion curves for the perfect quasi-1D waveguides are given in Figure 2, as a function of the normalized wave vector $\phi_x = k_x a$, where ϕ_x runs over the first Brillouin zone in the interval $[-\pi, \pi]$. *a* is the lattice parameter.

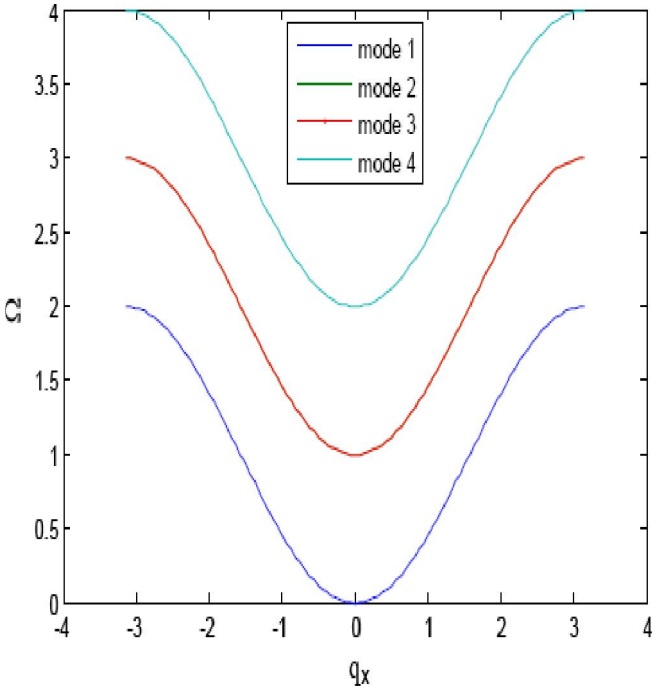

Figure 2 : Typical magnon dispersion curves for the perfect quasi-one-dimensional waveguide of Figure 1.

THE SCATTERING PROBLEM

To analyze the scattering on a waveguide in the presence of an atomic hole defect, as in Figure 1, it is essential to know the evanescent $|\eta_i| < 1$, as well as the propagating solutions $|\eta_i| = 1$, for a complete description of the scattering processes. Since the perfect waveguide does not couple between different eigenmodes, we can treat the scattering problem for each eigenmode separately.

For a magnon mode η_i, incident at a frequency Ω from the left to the right along the x-direction, the scattering outputs due to the nanocontact are coherent reflected and transmitted fields. The Cartesian components α of the displacement field $u\alpha(n, m, s)$ for an outside atom bordering the nanocontact domain, may be expressed using the matching approach as the sum of an incident propagating wave and a superposition of the reflected eigenmodes of the quasi-1D perfect waveguide at the same frequency. It may be written as

$$\mathbf{u}'\alpha\mathbf{(n, m, s) = u_i\eta_i^n + \Sigma_j\eta_j^{-n}R_{ij}u_j \text{ with } n < -2} \quad (6)$$

The vectors u_i and u_j denote the associated eigenvectors of the dynamic matrix for the perfect waveguides. In this equation R_{ij}, is the reflection amplitudes, into eigenmodes j = 1, 2, 3, 4 for the scattering at a given frequency Ω.

Whereas, for a site in the perfect waveguide (at the right of the nanocontact), the displacement field $u\alpha(n, m, s)$ is expressed by the superposition of the eigenmodes of the perfect waveguide

$$\mathbf{u\alpha(n, m, s) = \Sigma_j\eta_j^n T_{ij}u_j \text{ with } n > 2} \quad (7)$$

The quantities T_{ij} are the corresponding transmission amplitudes for the incident modes i = 1, 2, 3, 4 of the quasi-1D perfect waveguide.

Consider a Hilbert space constructed from the basis vectors [|R>, |T>] for the reflection and transmission into the different eigenmodes. Further, $|\zeta^{\pm}_p(\text{nanocontact})>$ is considered to group the spin precession displacements for an irreducible set of spins in the nanocontact domain, where $n \in [-2, +2]$. The equations of motion for this domain, coupled to the rest of the system, may be written in terms of the vector $[|\zeta^{\pm}_p(\text{nanocontact})>, |R>, |T>]$.

Use of the transformations connecting the spin precession displacements yields a square linear inhomogeneous system of equations of the form

$$\mathbf{[\Omega \mathit{I} - D(\{\eta_j\},\gamma)]\,[|\zeta^{\pm}_p(nanocontact)>, |R>, |T>] = -|IH, \eta_i>} \quad (8)$$

Where the vector $-|IH, \eta_i>$, mapped appropriately onto the basis vectors in the constructed Hilbert space, regroups the inhomogeneous terms describing the incoming magnon.

For non-trivial solutions for the components of the column vector $[|\zeta^{\pm}_p(\text{nanocontact})>, |R>, |T>]$, the determinant of the spin dynamics matrix $[\Omega I - D(\{\eta_j\},\gamma)]$ must vanish. This yields the energies of the localized spin states on the nanocontact domain.

In scattering phenomena the reflection and transmission effects are described in terms of the scattering matrix elements[21, 22], which are given explicitly by the reflection coefficient R_{ij} for the backward scattered or reflected waves j, and the transmission coefficient T_{ij} for the forward scattered or transmitted wave j, per incident propagating mode i.

The scattering behavior for the magnons is described, as for the coherent scattering of other excitations, in terms of the scattering matrix.

For different incident magnons i, the solutions of Eq.(8) yield the reflection and transmission coefficients R_{ij} and T_{ij} on the perfect waveguides, and the spin fluctuations vector $[|\zeta^{\pm}_p(\text{nanocontact})>$ for the irreducible set of spins. The reflection and transmission scattering cross sections r_{ij} and t_{ij} are then given at the scattering frequency Ω, as

$$\mathbf{r_{ij} = (v_{gj}/v_{gi})\,|R_{ij}|^2 t_{ij} = (v_{gj}/v_{gi})\,|T_{ij}|^2} \quad (9)$$

The scattering cross sections are normalized with respect to the group velocities of the magnons to obtain unitarity for the scattering matrix. v_{gi} is the group velocity of the eigenmode i, it is equal to zero for evanescent modes.

We can define total reflection and transmission cross sections for a given eigenmode i at frequency Ω, by summing over all the contributions of the scattered magnons

$$\mathbf{r_i(\Omega) = \Sigma_j r_{ij}(\Omega)\; t_i(\Omega) = \Sigma_j t_{ij}(\Omega)} \quad (10)$$

Furthermore, in order to describe the overall transmission of a mesoscopic multichannel system at a given frequency Ω, it is useful to define the total magnon conductance, or nanostructure transmittance, $\sigma(\Omega)$

$$\mathbf{\sigma(\Omega) = \Sigma_i\Sigma_j t_{ij}(\Omega)} \quad (11)$$

where the sum is carried out over all input and output channels at the frequency Ω.

NUMERICAL APPLICATIONS

In Figure 2 the dispersion branches for the magnons of the perfect waveguides are presented over the first Brillouin zone in the interval $[-\pi, \pi]$. The magnons labelled $i \in \{1, 2, 3, 4\}$, from bottom to the top in that order, are propagating modes in the respective frequency intervals: $\Omega_1 = [\Omega_{1,min} = 0, \Omega_{1,max} = 2.00]$, $\Omega_2 \equiv \Omega_3 = [\Omega_{2,min} = 1.00, \Omega_{2,max} = 3.00]$

Full Paper

and $\Omega_4 = [\Omega_{4,min} = 2.00, \Omega_{4,max} = 4.00]$.

There are one acoustical mode (1) and three optical modes (2, 3, 4). The modes 2 and 3 are degenerate. The acoustical mode (1) is characterized by the limiting behavior of his magnon branches, tending to zero frequency when the wavevector tends to zero, and the three optical modes their branches differ from zero in the long wavelength limit.

The configuration of the nanocontact, studied in this work, is presented in Figure 1. The scattering of the magnons at the nanocontact domain is studied with reference to incident spinwaves of the perfect waveguide, which is split into its transmitted and reflected parts. The results presented are obtained with reference to incident magnons from the left of the nanocontact domain to right in Figure 1. The numerical analysis is carried out for three possibilities: (*i*) $\gamma = 0.9$ (*ii*) $\gamma = 1.0$ (*iii*) $\gamma = 1.1$, which is a reasonable possibility (softening, homogeneous and hardening).

For $\gamma < 1$ ($\gamma > 1$), a magnetic softening (hardening) is said to take place on the nanocontact domain. For $\gamma = 1$, the local exchange is the same as throughout the system.

In Figure 3, we present the total magnon conductance of the system $\sigma(\Omega)$, is a useful quantity to calculate, as it corresponds to an experimentally measurable observable, for example in heat transfer, it induced by sum of the propagating modes of the system; it undergoes the influence of the variation of the parameters of the system at the neighbourhood of the nanocontact domain. It spreads on a beach of frequencies corresponding to $0 \le \Omega \le 4.00$, the magnon energy band; these curves of conductance varies according to parameter γ, and present peak resonances of different heights and widths, around frequencies $\Omega = 2.10$ and 2.10, what gives it a rough aspect.

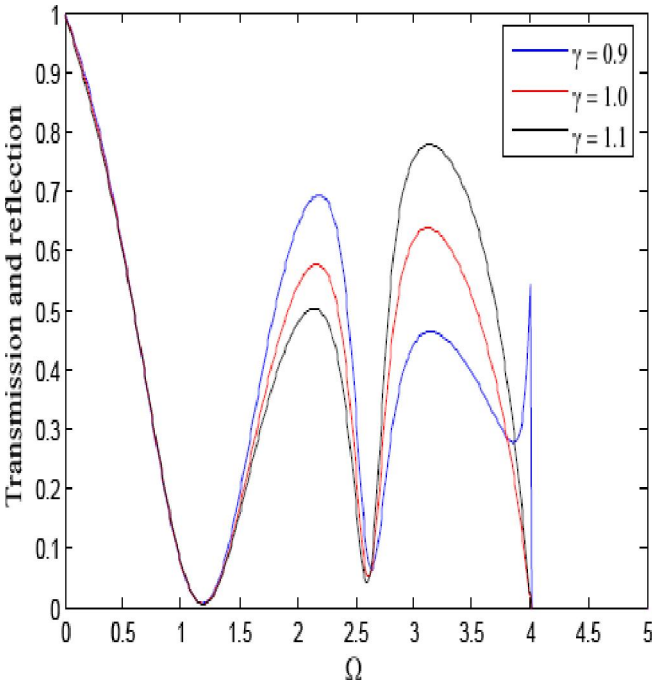

Figure 3 : The total magnon conductance, calculated in the frequency interval that covers the propagation of all the waveguide magnons.

The total magnon conductance, $\sigma(\Omega)$, is less than or equal to one magnon throughout the $\Omega \in [0, 4.00]$ interval. This illustrates how the atomic nanocontact at the heart of the contact domain constricts the transmission to a maximum of one magnon at a time, which is characteristic for the single-atomic chain $n \in [-2, +2]$. Another general characteristic of the total magnon conductance, in the interval $\Omega \in [1.20, 4.00]$, is the displacement of its spectral features to lower frequencies with increasing hardening of the magnetic exchange in the nanocontact domain. In the interval of frequency [0, 1.20], we observe the same behavior of magnon in the three considered cases of γ. At the frequency position $\Omega = 1.20$, the conductance presents his minimum and beyond this position, it presents two resonance positions. These resonances don't correspond to characteristic Fano resonances. These resonances are due to the interaction of the continuum with the localized spin precession states. We note also, the acoustic mode presents significant magnonic conductance, $\sigma(\Omega)$, for very low frequencies, for all three cases of exchange on the nanocontact domain, probably due to the relatively long wavelengths of the mode in this frequency interval, in comparison with the lattice parameter, and also due to the absence of interference effects on the nanocontact with the two other high energy optic modes.

The model is applied to calculate numerically the energies of localized spin states in the neighborhood of the nanocontact domain joining the two semi-infinite quasi-1D lattices. These spin states demonstrate the essential features of the spinwave nanocontact modes and the influence of perfect-perturbed zone interaction parameters on the localized modes of magnons at the nanocontact domain. The spinwave dispersion curves for the perfect system and nanocontact modes are shown

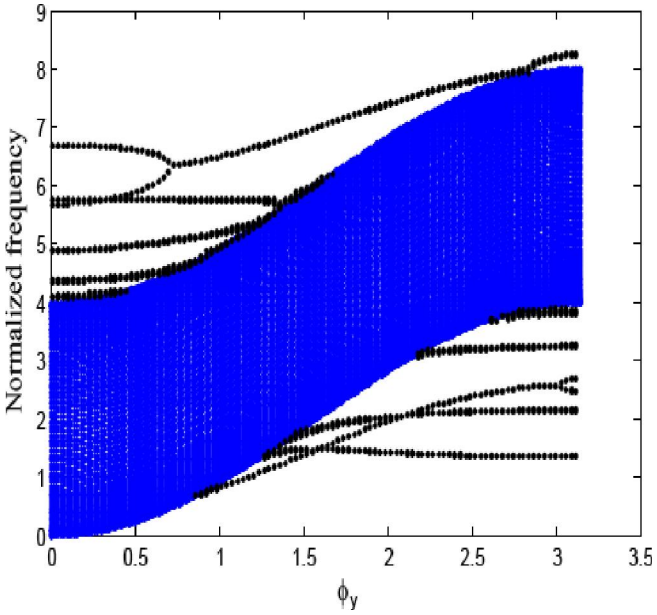

Figure 4a : Localized spinwave dispersion branches on the nanocontact domain between two identical semi-infinite quasi-1D structures. The dispersion relations correspond to a softening case $\gamma = 0.9$. The shaded area represents the propagating modes for the perfect quasi-1D system.

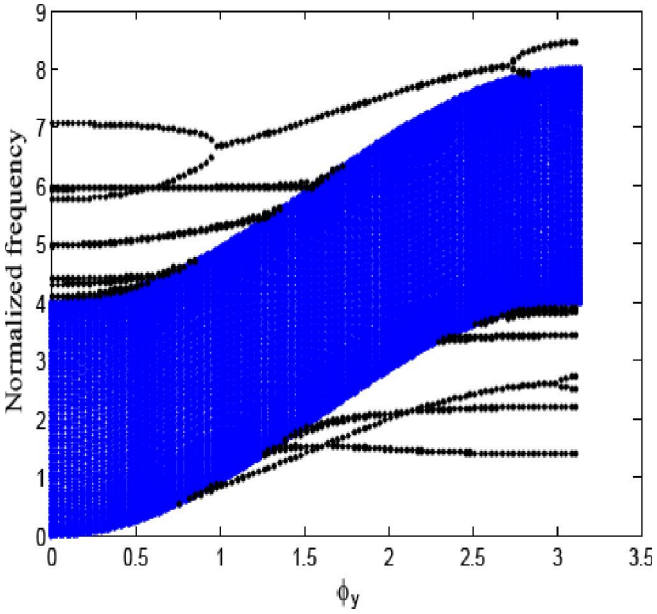

Figure 4b : Localized spinwave dispersion branches on the nanocontact domain between two identical semi-infinite quasi-1D structures. The dispersion relations correspond to a homogeneous case $\gamma = 1.0$. The shaded area represents the propagating modes for the perfect quasi-1D system.

in Figures 4(a, b, c), as a function ϕ_y, propagating parallel to the nanojunction zone. As pointed out earlier these dispersion branches represent the propagating part of the localized spin states that otherwise decay into the bulk of the perfect lattices along the x-direction.

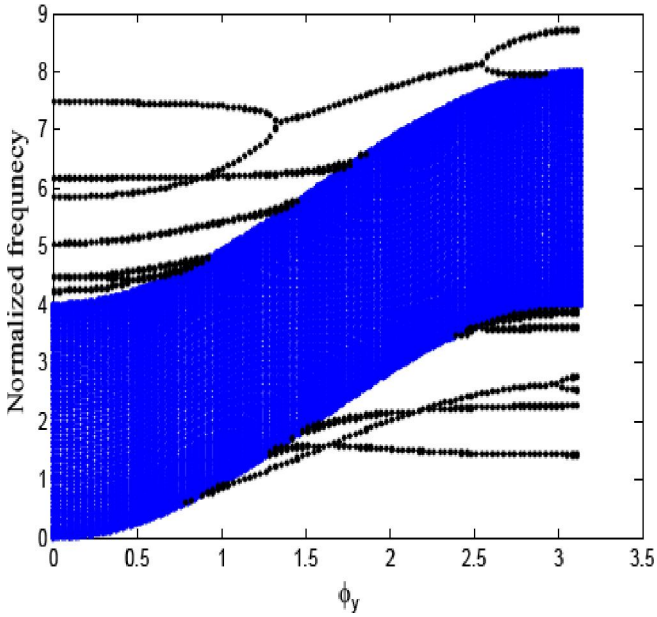

Figure 4c : Localized spinwave dispersion branches on the nanocontact domain between two identical semi-infinite quasi-1D structures. The dispersion relations correspond to a hardening case $\gamma = 1.1$. The shaded area represents the propagating modes for the perfect quasi-1D system.

As has been mentioned, the regions where $|\eta_i| = 1$ correspond to the propagating modes for the perfect semi-infinite waveguides regions as shown in shaded area in Figures 4(a, b, c). Near the nanocontact region, the dispersion curves depict magnons propagating along the x-direction that are however effectively localized in the sense that their spin fluctuation field is evanescent in the chains normal to the nanocontact. The amplitude of the localized spinwave in the nanocontact zone decays exponentially with increasing penetration into the two semi-infinite perfect quasi-1D waveguides. These localized spin states are dynamic spin states for which the spin precession field decreases in amplitude with distance from the nanocontact domain into the chains, in conformity with the evanescent modes on the chains. Their energies displace, naturally, to higher frequencies with increasing magnetic exchange in the nanocontact domain.

Let us mention that in Figure 4a, the softening case is considered, whereas in Figure 4b the same exchange interactions are taken everywhere. In the Figure 4c, the hardening case is presented. Comparison between the three Figures (4a, 4b, 4c), one notes that the localized branches shift towards the high frequencies with the hardening of the magnetic exchange in the nanocontact

Full Paper

domain and become more energetic, in all examined cases. For example, for $\phi_y = 0$, $\Omega_{max} = 6.75$ (in Figure 4a); $\Omega_{max} = 7.00$ (Figure 4b); $\Omega_{max} = 7.50$ (Figure 4c).

In conclusion, we have presented a model calculation for the study of the coherent magnon transmission via an atomic nanocontact which acts as the joint between two sets of semi-infinite quasi-1D monatomic chains. The analysis of the conductance spectra and localized spin sates of the set of irreducible sites in the nanocontact domain demonstrate the central role of a core subset of these sites for the dynamics of the system. The fluctuations observed in the localized spin states spectra are effectively due to the interaction between the incident propagating modes with the scattered spinwaves of the system, effects that are induced by the modification of boundary magnetic exchange values. At this time, experimental or simulated data are not available to compare with our results. The numerical results yield an understanding for the relation between the coherent magnon conductance and the geometric of the nanocontact in the perfect quasi-1D system. It can also serve towards the study of granular chains constructed in an analogous manner on the classical macroscopic scale.

REFERENCES

[1] C.Giardina, R.Livi, A.Politi, M.Vassalli; Phys.Rev.Lett., **84**, 2144 **(2000)**.

[2] O.V.Gendelman, A.V.Savin; Phys.Rev.Lett., **84**, 2381 **(2000)**.

[3] K.Saito, S.Takesue, S.Miyashita; Phys.Rev., **E54**, 2404 **(1996)**.

[4] X.Zotos, F.Naef, P.Prelovs˘ek; Phys.Rev., **B55**, 11029 **(1997)**.

[5] V.Shchukin, D.Bimberg; Rev.Mod.Phys., **71**, 1125 **(1999)**.

[6] K.Kern, H.Niehaus, A.Schatz, P.Zeppenfeld, J.Goerge, G.Comsa; Phys.Rev.Lett., **67**, 855 **(1991)**.

[7] B.Gambardella, M.Blanc, L.Burgi, K.Kuhnke, K.Kern; Surf.Sci., **449**, 93 **(2000)**.

[8] S.Rousset et al.; Materials Sc.Eng., **B96**, 169 **(2002)**.

[9] P.Gambardella, A.Dallmeyer, K.Maiti, M.C.Malagoli, S.Rusponi, P.Ohresser, W.Eberhardt, C.Carbone, K.Kern; Phys.Rev.Lett., **93**, 077203 **(2004)**.

[10] N.Weiss, T.Cren, M.Epple, S.Rusponi, G.Baudot, A.Tejeda, V.Repain, S.Rousset, P.Ohresser, F.Scheurer, P.Bencok, H.Brune, Phys.Rev.Lett., **95**, 157204 **(2005)**.

[11] A.Vindigni, A.Rettori, M.G.Pini, C.Carbone, P.Gambardella; Appl.Phys., **A82**, 385 **(2006)**.

[12] T.Wolfram, R.E.DeWames, in: S.G.Davison (Ed), Progress in Surface Science, **2**, **(1972)**.

[13] F.Schütz, M.Kollar, P.Kopietz; Phys.Rev.Lett., **91**, 017205 **(2003)**.

[14] D.L.Mills; Phys.Rev., **B40**, 11153 **(1989)**.

[15] I.D.Paczek, N.N.Chen, M.G.Cottam; Phys.Rev., **B45**, 12898 **(1992)**.

[16] M.Abou Ghantous1, A.Khater; Eur.Phys.J., **B12**, 335 **(1999)**.

[17] R.Tigrine, A.Khater, B.Bourahla; Eur.Phys.J., **B62**, 59 **(2008)**.

[18] A.Khater, R.Tigrine, B.Bourahla; Phys.Status Solidi., **B246**, 1614 **(2009)**.

[19] A.Khater, B.Bourahla, R.Tigrine, M.Abou Ghantous; Eur.Phys.J., **B82**, 1 **(2011)**.

[20] A.Khater, M.Abou Ghantous; Surf.Sci.Lett., **498**, L97 **(2002)**.

[21] R.Landauer; Philos.Mag., **21**, 863 **(1970)**.

[22] M.Büttiker; Phys.Rev.Lett., **57**, 1761 **(1986)**.